VARIABLE-ORDER STOCHASTIC ADAPTIVE CONTROL OF ROBOTIC MANIPULATORS WITH A FLEXIBLE FOREARM

Yee-Pien Yang and Yung-Chuan Chu
Department of Mechanical Engineering
National Taiwan University
Taipei, Taiwan 107, R.O.C.

Abstract

An application of recursive covariance lattice filter to the adaptive estimation and stochastic control of a robotic manipulator with one flexible link is presented. Not only the effective order, but also the corresponding parameters of an AutoRegression Moving Average with a Bias (ARMAB) prediction model of the manipulator are updated by a set of pure order recursive lattice algorithms. The reduced-order prediction model that represents significant dynamics of the plant is used to generate optimal control sequences by minimizing the expectation of a weighted cost functional. In the simulations, the manipulator is modeled by the finite element method and Lagrange's equations. The performance and robustness of the variable order stochastic adaptive controller are demonstrated by numerical results.

1. Introduction

The design and control of light weight robotic manipulators attracted much attention in the past decade. Plenty of research has been conducted on the adaptive control of manipulators with flexible links [1-4]. Recently, some literature dealt with the stochastic adaptive control of robotic manipulators with flexible links [9,10]. All but a few publications mentioned the order updating of the prediction model in the adaptive control of a flexible structure. Sundararajan and Montgomery [7] were first to apply lattice filters to the identification and adaptive modal control of flexible structures. This class of lattice algorithms has fast convergence rate and has many advantages over conventional least-squares algorithms. Besides its recursive property in both time and order, there exist orthogonalizing property, good tracking performance, rapid start-up capability, fast convergence and easy implementation due to its high repetitive structure. The extension of the original AR lattice form to the ARMA models by the embedding technique makes the lattice filter a very promising perspective in the control framework [8,9].

This paper presents an application of the recursive covariance lattice filter [10] to the stochastic adaptive control of a robotic manipulator with one rigid link and one flexible link in the gravitational field, considering various measurement noises. The adaptive control scheme is indirect; i.e., the control signal at each sampling instant is based on an output prediction model of the plant. This prediction model is in a linear ARMAB form with time-varying parameters. The recursive covariance lattice filter is applied to estimate the effective order of the ARMA part of the prediction model to reflect the most significant dynamics (or modes) of the plant, as well as to estimate the corresponding parameters. The most attracting feature of this filter is that the algorithm structure is a pure order recursive lattice of a set of generalized residual energy matrices. Therefore, the round-off errors will not propagate in the time direction as the conventional lattice filter does through time update of a cross-residual energy matrix. Thus the numerical inaccuracy and instability problems [11] caused by round-off errors are absent. The other important aspect of the proposed adaptive estimation process is the vector-channel embedding technique [12] to treat the moving average part of the ARMA model as an additional measurement channel. The bias in the ARMAB model is regarded as the ensemble average or the expectation of the output prediction error process, and is approximated by passing this random process through a low-pass filter.

The adaptive controller is designed to minimize the expectation of a weighted measure of control effort and the error between the system predicted output and the output of a reference model obtained from an optimal linear regulator problem. This error is made to decay according to an error dynamics model. Owing to the noncolocated sensors and actuators on the manipulator, the transfer function of the linearized plant model is non-minimum phase. Therefore, the plant becomes unrobust and sensitive to the perturbation of control parameters, for example, the weighting matrices of the cost functional. We found that a PD controller in an inner loop can augment the plant to produce stable discrete-time transmission and channel zeros. thereby improving robustness.

2. Manipulator Dynamics Model

The two-link manipulator to be controlled in a vertical plane of the gravity field is displayed schematically in Figure 1. Centered at o_1 and o_2 are two actuators modeled as rigid discs with the same mass M_1. Both of these actuators are ideal with infinity bandwidth and constant gain. The first link of mass M_L and length L is uniform, rigid and clamped to the first disc; the second link of the same mass and length is a uniform Euler-Bernoulli beam, clamped to the second disc. Them end-effector and the payload are modeled as a point mass M_2 at the other end of the second link. A control torque u_1 acts on the first disc, and a control torque u_2 acts between the second link and the second disc.

We use the finite element method to model the flexible link, which is approximated with three elements of equal length and cubic B-splines as interpolation functions. With the two rigid-body degrees of freedom, there are 5 degrees of freedom in the simulation model. The generalized displacement vector in the finite element model is $\eta = [\alpha_1\ \alpha_2\ y_1\ y_2\ y_3]^T \in \mathcal{R}^5$ where α_1 and α_2 are rigid angles and y_1, y_2, y_3 are the transverse elastic displacements of node 1, 2 and 3 on the second link. The cross section of the flexible link is rectangular with wider length in the out-of-plane direction so that the flexible link is relatively rigid in the out-of-plane motion, which is then negligible.

It is straightforward to write the kinetic energy, strain energy and gravitational potential energy for the finite element model of the manipulator, including the strain energy due to the inertial axial load. Lagrange's equations for the finite element model are derived as follows [13]:

$$M(\eta)\ddot{\eta} + D\dot{\eta} + [K + K_a(\eta, \dot{\eta}, \ddot{\eta}) - M_a(\dot{\alpha}_1 + \dot{\alpha}_2)^2]\eta + N(\eta, \dot{\eta}) = Bu \quad (1)$$

where $M(\eta)$ is a positive definite symmetric mass matrix, including the conventional consistent mass matrix and the

nonlinear inertia matrix involving second-order derivatives of the system coordinates, K is the nonnegative symmetric stiffness matrix due to bending stiffness of the flexible link, $N(\eta, \dot{\eta})$ is a vector containing nonlinear functions of various gravity, inertial torques and Coulomb frictions, B is the input influence matrix with 0's and 1's, and $u = [u_1\ u_2]^T$. The matrix $K_a(\eta, \dot{\eta}, \ddot{\eta})$, namely the geometric stiffness matrix, represents the effect of the inertial axial load on the transverse vibration of the second link, which is obtained from the virtual work done by the nonconservative axial load, and is then an explicit function of rigid angular velocities and angular acceleration s of the manipulator links. The term $M_a(\dot{\alpha}_1 + \dot{\alpha}_2)^2$ is derived from part of the kinetic energy of the second link, which accounts for the effect of the centrifugal force component in the direction perpendicular to the undeformed position of the flexible link, thereby reducing the stiffening effect of the inertial axial load. The damping matrix D is 10^{-6} times the part of the mass matrix that corresponds to the flexible link if α_1 and α_2 are held constant; this means that we model small proportional structural damping for the flexible link. System parameters are listed in Table 1.

Table 1: System parameters

l = length of each link = 1.5 m
r = radius of each joint = 0.05 m
m = mass of each link = 1.2465 kg
M_1 = mass of each disc = 62.325 g
M_2 = mass of payload
EI of the flexible link = 399 Nm^2
a = cross section height = .015 m
b = cross section width = .020 m

3. Output Prediction Model

Consider a digital control of (1) with zero-order sample and hold devices with a sampling time h. The output vector $y(k) \in \mathcal{R}^m$ (m=3) is measured at the beginning of the kth sampling interval (k=0,1,2,...) or at time kh, and the constant control vector $u(k) \in \mathcal{R}^r$ ($r = 2$) is applied for the duration of the kth sampling interval. We take

$$y(k) = [\alpha_1(k)\ \alpha_2(k)\ y_3(k)]^T \tag{2}$$

where α_1 and α_2 are the rigid-body angles and y_3 is the transverse elastic tip deflection, measured from the undeformed position, of the flexible link that holds the payload.

To simulate the measurement noise process, we assume various measurement error model in measuring the tip displacement of the flexible link and rigid angle of each joint. The tip displacement measurement sensor, a camera or a laser displacement meter, is corrupted with additive random white Gaussian noise ς_y, characterized by mean 0 and covariance σ^2. The angular displacement of each joint is measured by digital encoder of P pulses per revolution, whose measurement error $\varsigma_{\alpha i}$ (i=1, 2) is modeled to be +1, 0 or -1 pulse with equal likelihood (1/3). That means the probability density function of the measurement error of each encoder is discrete. Thus the actual measurements model is

$$y_F(t) = [\alpha_1(t)\ \alpha_2(t)\ y_3'(t)]^T + \varsigma(t) \tag{3}$$

where $\{y_3'(t)\}$ is a sequence of the filtered output of $\{y_3(t)\}$, passing through a low-pass filter, and $\varsigma = [\varsigma_{\alpha 1}, \varsigma_{\alpha 2}, \varsigma_y]^T$ is a 3-vector of measurement noise which is assumed independent of the process noise v and of the system initial states.

Based on the standard linear system theory, the corresponding input/output model for (1) and (3) with digital input and output has the form of the multivariable autoregression moving average with a bias (ARMAB) model

$$y_F(k) = A(k, q^{-1})y_F(k) + B(k, q^{-1})u(k) + m_b(k) \tag{4}$$

where q^{-1} is a backward shift operator, m_b accounts for the modeling bias due to gravity effects and unmodeled dynamics, and $A(k, q^{-1})$ and $B(k, q^{-1})$ are polynomial matrices of order $N(\leq 10)$.

For any completely observable linear system, properly located sensors observe the same dynamics of the system. Therefore, the matrices A_i's in (4) can be replaced by scalars a_i's which are coefficients of the system characteristic polynomial. In this paper, however, the two-link robotic manipulator with a flexible arm is very nonlinear. This motivates us to use two vector-channel auto-regressive models for two independent estimation channels, each for one link.

The first estimation channel for the rigid link consists of the first rigid angle α_1 and two inputs u_1 and u_2; the second estimation channel for the flexible link consists of the second rigid angle α_2, filtered tip displacement y_3' and the two inputs. Both estimation channels have the same AR model form with bias, i.e.,

$$\begin{aligned} z_l(k) &= \sum_{j=1}^{N} \begin{bmatrix} a_{lj}(k) & B_{lj}(k) \\ C_{lj}(k) & D_{lj}(k) \end{bmatrix} z_l(k-j) + \begin{bmatrix} m_{bl}(k) \\ n_{bl}(k) \end{bmatrix} \\ &= \sum_{j=1}^{N} A_{l,N,j}(k) z_l(t-j) + \xi_l(t), \qquad l = 1, 2 \end{aligned} \tag{5}$$

where

$$z_1 = \begin{bmatrix} \alpha_1 \\ u_1 \\ u_2 \end{bmatrix}, \qquad z_2 = \begin{bmatrix} \alpha_2 & y_3' \\ u_1 & 0 \\ u_2 & 0 \\ 0 & u_1 \\ 0 & u_2 \end{bmatrix} \tag{6}$$

and C_{lj} and D_{lj} are two auxiliary matrices. It is apparent that the first rows of $A_{l,N,j}$ contain all the original ARMA coefficients, and ξ_l represents the prediction error vector of the lattice filter.

4. The Recursive Covariance Lattice Filter

4.1 General Description of Lattice Filters

Let the Hilbert space $H_l(k)$ be spanned by the history process $\{z_l(k) \in \mathcal{R}^{p_l \times m_l}\}$, where the $p_l \times m_l$ matrix z_l amounts to p_l subchannels, each of which contains m_l scalar measurements. The subscription l denotes the lth main estimation channel, for link l. Without loss of generality, we omit the subscription l for simplicity. For each estimation channel of the robot arm, we further let $H_n^i(k)$ be a closed subspace of $H(k)$ spanned by $Z_{t-n}^{t-i} = \{z(k-n), ..., z(k-i-1), z(k-i)\}$, $1 \leq i \leq n$. In this subspace we define $P_n^i(k)$ as the orthogonal projection operator onto $H_n^i(k)$ [12]. The basic idea of the lattice algorithm is to construct a set of orthogonal basis vectors for $H_n^1(k)$ to replace the original history process $\{z_l(k)\}$.

Then, we define the forward and backward residual error vectors for each main estimation channel (Actually, the 'vector' is an $p \times m$ matrix or vector array) :

$$f_0(k-n) \triangleq z(k-n)$$
$$f_i(k-n+i) \triangleq [I - P_n^{n-i+1}(k)]z(k-n+i), \quad i = 1, ..., n \tag{7}$$

and

$$b_0(k-1) \triangleq z(k-1)$$
$$b_i(k-1) \triangleq [I - P_i^1(k)]z(k-i-1), \quad i = 1, ..., n-1. \tag{8}$$

These can be readily achieved by using the Gram-Schmidt orthogonalization of the history space. It has been shown in [10] that the lattice equations for residual errors are

$$f_{n+1}(k) = f_n(k) + K_{n+1}^f(k)b_n(k-1), \; f_0(k) = z(k) \tag{9}$$

$$b_{n+1}(k) = b_n(k-1) + K_{n+1}^b(k)f_n(k), \; b_0(k) = z(k) \tag{10}$$

where K_n^f and K_n^b are respectively called the forward and backward reflection coefficient matrices of dimension $p \times p$. These reflection matrices are so obtained that they minimize the residual energy matrices

$$R_n^f(k) \triangleq f_n(k)f_n^T(k) \tag{11}$$

and

$$R_n^b(k) \triangleq b_n(k)b_n^T(k). \tag{12}$$

Likewise, the cross residual energy matrix is defined by

$$C_n(k) \triangleq f_n(k)b_n^T(k-1). \tag{13}$$

Thus the reflection matrices can be adjusted through some algebra:

$$K_n^f(k) = -C_{n-1}(k)R_{n-1}^{-b}(k-1) \tag{14}$$
$$K_n^b(k) = -C_{n-1}^T(k)R_{n-1}^{-f}(k). \tag{15}$$

Substituting (9), (10), (14) and (15) into (11) and (12) yields order update equations for R_n^f and R_n^b as follows:

$$R_{n+1}^f(k) = R_n^f(k) + K_n^f(k)C_n^T(k) \tag{16}$$
$$R_{n+1}^b(k) = R_n^b(k-1) + K_n^b(k)C_n(k). \tag{17}$$

However, there exists no order update for the cross residual energy matrix $C_n(k)$. To close the lattice filter loop, we need to derive the time-update equation for $C_n(k)$. This causes the accumulation of round-off errors from calculation of the forward and backward error vectors in the time direction. To avoid this defect, Strobach [10] proposed a generalized covariance lattice technique called the pure order recursive lattice algorithm method.

4.2 Pure Order Recursive Covariance Lattice Algorithm

The pure order recursive lattice algorithm method is developed for AR system identification problems by expanding the residual matrix (11)-(13) to the generalized residual energy matrices in block matrix forms as follows:

$$R_{n,i,j}^f(k) = f_n(k-i)f_n^T(k-j) \tag{18}$$
$$R_{n,i,j}^b(k) = b_n(k-i-1)b_n^T(k-j-1) \tag{19}$$
$$C_{n,i,j}(k) = f_n(k-i)b_n^T(k-j-1). \tag{20}$$

Since symmetric properties and shift invariance properties holds for the generalized residual matrices, substituting (9)-(10) into (18)-(20) leads to four recursive equations which complete the order-recursive covariance lattice loop:
At the sampling instant k,
for $n = 1, N-1$,
for $j = 0, N-n-1$,
N: order of the algorithm or order of the autoregression with bias model (5),

$$\begin{aligned} R_{n,0,j}^f(k) &= R_{n-1,0,j}^f(k) + K_n^f(k)C_{n-1,j,0}^T(k) \\ &\quad + C_{n-1,0,j}(k)K_n^{f^T}(k-j) \\ &\quad + K_n^f(k)R_{n-1,0,j}^b(k)K_n^{f^T}(k-j) \end{aligned} \tag{21}$$

$$\begin{aligned} R_{n,0,j}^b(k) &= R_{n-1,0,j}^b(k-1) + K_n^b(k-1)C_{n-1,0,j}(k-1) \\ &\quad + C_{n-1,j,0}^T(k-1)K_n^{b^T}(k-j-1) \\ &\quad + K_n^b(k-1)R_{n-1,0,j}^f(k-1)K_n^{b^T}(k-j-1) \end{aligned} \tag{22}$$

$$\begin{aligned} C_{n,0,j}(k) &= C_{n-1,0,j+1}(k) + K_n^f(k)R_{n-1,0,j+1}^b(k) \\ &\quad + R_{n-1,0,j+1}^f(k)K_n^{b^T}(k-j-1) \\ &\quad + K_n^f(k)C_{n-1,j+1,0}^T(k)K_n^{b^T}(k-j-1) \end{aligned} \tag{23}$$

$$\begin{aligned} C_{n,j+1,0}(k) &= C_{n-1,j,0}(k-1) + R_{n-1,j,0}^f(k-1)K_n^{b^T}(k-1) \\ &\quad + K_n^f(k-j-1)R_{n-1,j,0}^b(k-1) \\ &\quad + K_n^f(k-j-1)C_{n-1,0,j}^T(k-1)K_n^{b^T}(k-1) \end{aligned} \tag{24}$$

The convergence conditions for the lattice algorithm are the same as those for the recursive least squares method, as investigated in [14].

4.3 AR Coefficients and Order Determination

The coefficients $a_{ki}(k)$ and $B_{ki}(k)$ in the autoregression part of (5) with an effective order are required to generate optimal adaptive control signals. Recall that $f_n(k)$ is the error remaining after orthogonal projection of the data taken through time k onto the history space $H_n^1(k)$, i.e.,

$$f_n(k) = z(k) - \sum_{j=1}^{n} \mathcal{A}_{n,j}(k)z(k-j) \tag{25}$$

and the coefficient matrices $\mathcal{A}_{n,j}(k)$ minimize the H_n^1 norm of $f_n(k)$ over all AR models of order n. Similarly,

$$b_n(k) = -\sum_{j=0}^{n-1} \mathcal{B}_{n,j}(k)z(k-j) + z(k-n). \tag{26}$$

Manipulating (9)-(10) with (25)-(26), we obtain the following equations

$$\mathcal{A}_{n,j}(k) = \mathcal{A}_{n-1,j}(k) + K_n^f(k)\mathcal{B}_{n-1,j-1}(k-1) \tag{27}$$

$$\mathcal{B}_{n,j}(k) = \mathcal{B}_{n-1,j-1}(k-1) + K_n^b(k)\mathcal{A}_{n-1,j}(k) \qquad (28)$$
$$n = 2, ..., N, \quad j = 1, ..., n-1$$

given the initial and terminal conditions

$$\begin{aligned} \mathcal{A}_{n,0}(k) &= I \quad \mathcal{A}_{n,n}i(k) = -K_n^f(k) \\ \mathcal{B}_{n,0}(k) &= -K_n^b(k) \quad \mathcal{B}_{n,n}(k) = I. \end{aligned} \qquad (29)$$

It is apparent that the estimates of a_i and B_i are in the first rows of $\mathcal{A}_{n,j}$, $j = 1, ..., n$. From (4) and (5), the output prediction $\hat{y}(k+1)$ at one-step ahead of k can then be expressed as

$$\hat{y}_F(k+1) = \sum_{i=1}^{N} \left[\hat{A}_i(k) y_F(k-i+1) + \hat{B}_i(k) u(k-i+1)\right] + \hat{m}_b(k+1), \qquad (30)$$

where

$$\hat{A}_i = \begin{pmatrix} \hat{a}_{1i} & 0 & 0 \\ 0 & \hat{a}_{2i} & 0 \\ 0 & 0 & \hat{a}_{2i} \end{pmatrix} \qquad \hat{B}_i = \begin{pmatrix} \hat{B}_{1i,1} & \hat{B}_{1i,2} \\ \hat{B}_{2i,1} & \hat{B}_{2i,2} \\ \hat{B}_{2i,3} & \hat{B}_{2i,4} \end{pmatrix},$$

$\hat{B}_{li,j}$ denotes the jth element of the row vector $\hat{B}_{li}$.

The bias $\hat{m}_b(k+1) = E[y_F(k+1) - y_F(k+1)]$ is estimated by passing the filtered output prediction error through a first-order low-pass filter of corner frequency at 5 Hz. In our adaptive control process, the effective order of the ARMAB model at time k is N if

$$ln\ R_{N,0,0}^f(1,1) < \epsilon \qquad (31)$$

where ϵ is chosen as a small positive real number.

5. Adaptive Controller Algorithm

The reduced-order controller is based on the certainty equivalent principle. The adaptive control signal is determined by setting the predicted output from the reduced-order prediction model (30) equal to a desired output. The desired output y_d is defined so that the error between the desired output and a reference signal y_r decays according to an error dynamics model

$$y_d(k+1) = y_r(k+1) - a_e(k)[y_F(k) - y_r(k)] \qquad (32)$$

where

$$a_e(k) = (a_0 - a_f)\beta^k + a_f \qquad (33)$$

with a_0, a_f and β positive scalars less than 1. The optimal one-step-ahead control u_a is obtained by minimizing the quadratic functional

$$J(k) = E\{\|y_F(k+1) - y_r(k+1) + a_e(k)[y(k) - y_r(k)]\|_Q^2 + \|u_a(k)\|_{R_1}^2 + \|u_a(k) - u(k-1)\|_{R_2(k)}^2 | \mathcal{F}_k\} \qquad (34)$$

where Q is a nonnegative diagonal matrix; R_1 and $R_2(k)$ are positive definite diagonal matrices with

$$R_2(k) = R_{20}\gamma^k \qquad (35)$$

for some nonnegative γ less than 1; $\mathcal{F}_k$ denotes the sigma algebra generated by $\{y_F(k), y_F(k-1), ..., y_F(0)\}$. The time-varying $R_2(k)$ is very important to prevent control chattering as discussed in [3].

The first two components of the reference signal y_r are computed off-line. These components are the outputs of two second-order reference models chosen to ensure that y_r represents a reasonable response for a system with two rigid-body modes. The authors solved an optimal linear regulator problem for each of the two uncoupled second-order systems to obtain two uncoupled linear reference models that produced the reference signal α_{1r} and α_{2r} in Figures 3 and 4. The third component of y_r is an estimated static tip deflection under gravity; i.e., the measured tip deflection is fed into a first-order low-pass filter with a corner frequency at 4 Hz and the output of this filter is used as the tip reference signal. The discrete-time transfer function of the low-pass filter is

$$T(z) = \frac{1-\kappa}{z-\kappa}, \qquad (36)$$

where $\kappa = \exp(-\omega_c h)$, h = sampling time = 0.01 sec, and the corresponding corner frequency ω_c is 4 Hz. Robustness can be improved by augmenting the plant with an inner continuous-time PD control loop with the transfer function $T_{pd}(s)$ as shown in Figure 2. The total control signal $u(k)$ is, therefore, the combination of the adaptive control signal $u_a(k)$ and the proportional and derivative control signal $u_{pd}(k)$.

6. Simulations

The nonlinear response of the robot motion was simulated on IBM 3090 supercomputer by solving the equations of motion in (1) with a fourth-order Runge-Kutta algorithm with variable step size. The flexible link of the manipulator is modeled by three finite elements, thus the system order is 10. The adaptive controller drives the manipulator in the vertical plane under gravity through two working phases. For the first working phase, the manipulator moves from the horizontal position ($\alpha_1 = 90°$, $\alpha_2 = 0°$) to the position $\alpha_1 = 135°$, $\alpha_2 = 45°$, grasping a payload; then the manipulator is moved to the position $\alpha_1 = 180°$, $\alpha_2 = 90°$ in the the second working phase. A learning period about 45 samples was found essential before the robot motion for a converged set of parameters in the prediction model, in which the control torques were constrained not to exceed 1.5 times the magnitudes of the initial torques holding the links at the horizontal position; but no more learning was necessary for the second working phase.

The inner loop PD controller design is based on gravity torques and a rigid-body mass matrix that are 40% greater than their correct values for no payload. The proportional and derivative gain matrices, designed according to [15], are

$$K_p = \begin{bmatrix} 266793 & 82267 \\ 82267 & 49114 \end{bmatrix} \quad K_d = \begin{bmatrix} 896862 & 27234 \\ 27234 & 13807 \end{bmatrix}. \qquad (37)$$

This PD controller alone cannot guarantee consistently good control performance for large motions of the manipulator. Therefore, most of the control effort has been provided by the adaptive control law $u_a(k)$.

The covariance of the measurement noise for the tip displacement is $.001^2$. The digital encoder on each joint has 1000 pulse per revolution, then the accuracy is $\pm 2\pi/1000$ rad. Other control parameters in (32)-(35) are

$$Q = \text{diag}[35, 30, 0.07], \quad R_1 = \text{diag}[3.5 \times 10^{-5}, 3.5 \times 10^{-5}] \qquad (38)$$

During the learning period:

$$a_0 = 0.98,\ a_f = 0.7,\ \beta = 1$$
$$R_{20} = \mathrm{diag}[6.5 \times 10^{-3},\ 3.5 \times 10^{-2}],\ \gamma = 1 \qquad (39)$$

After learning period:

$$a_0 = 0.98,\ a_f = 0.7,\ \beta = e^{-0.007}$$
$$R_{20} = \mathrm{diag}[2.0 \times 10^{-5},\ 2.0 \times 10^{-4}],\ \gamma = 0.1^{0.01} \qquad (40)$$

Based on the physical realization of robot system dynamics — nonlinearly coupled rigid-body and flexible motions, the minimum and maximum effective order of each lattice estimation channel can be assigned before the adaptive parameter estimation. The minimum effective order for both channels is fixed as 4, which accounts for two rigid body modes. The maximum effective order is 6 for channel one and 8 for channel two, each including extra excited flexible modes. The upper bound ϵ in (31) for the order determination is set at -5 and -4 for the first and second channel, respectively.

Figures 3 and 4 show the adaptive control performance for the manipulator without payload mass in the first working phase, but with a payload weighing 40 percent of the flexible link mass in the second working phase. Initially, the orders of two main estimation channels are both assigned at 4. At the steady state of the first working phase, the order of the first estimation channel settles at 6, while the order of the second channel varies up to order 8, then reducing to 6 as the first flexible mode dominates. After the robot grasps a payload, the order remains at 6 in the first channel, but rises to 8 in the second channel. This implies that the payload mass reduces the system stiffness, and so more modes are required to describe the system response.

7. Summary and Conclusions

An application of adaptive lattice estimation and stochastic control scheme to a two-link robotic manipulator with one flexible forearm has been presented. Though the simulation model of the manipulator is highly nonlinear, the stochastic adaptive digital controller that is based on a variable-order time-varying prediction model gives robust performance in response to changes in the plant dynamics corrupted with measurement noises. The combination of elastic vibrations and nonlinearities due to fast large-angle rigid-body motion necessitated two vector estimation channels and a bias compensation for the controller presented in this paper. The recursive covariance lattice filter with the vector-channel embedding technique has a pure order recursive property, which enables the lattice filter to identify the effective order of the prediction model for the plant and the corresponding parameters. Implemented inside the stochastic adaptive control loop were an error dynamics model, a time-varying weighting matrix on control variations, a continuous-time PD controller, a bias estimator and a low-pass filter used to estimate the steady-state static tip deflection. The simulations showed a fast convergence rate of the recursive covariance lattice algorithm, and fast tracking ability of the proposed stochastic adaptive controller. The numerical results also showed that the resulting closed loop system was robust to the unmodeled dynamics and measurement noises.

8. References

[1] Koivo, A. J. and Lee, K. S., "Self-Tuning Control of Planar Two-Link Manipulator With Non-Rigid Arm," *Proc. of 1989 IEEE Intl. Conf. on Robotics and Automation*, pp.1030-1035.

[2] Ronver, D. M. and Franklin, G. F., 1988, "Experiments in Load-Adaptive Control of a Very Flexible One-Link Manipulator," *Automatica*, Vol. 24, No. 4, pp.541-548.

[3] Yang, Y. P. and Gibson, J. S., 1989, "Adaptive Control of a Robotic Manipulator with a Flexible Arm," *Journal of Robotic Systems*, Vol.6(3), June, pp.271-232.

[4] Yurkovich, S., Tzes, A. P., Lee, I. and Hillsley, K. L., 1990, "Control and System Identification of a Two-Link Flexible Manipulator," *Proceedings of IEEE International Conference on Robotics and Automation*, pp.1626-1631.

[5] Oakley, C. M. and Cannon, R. H., 1989, "End-Point Control of a Two-Link Manipulator with a Very Flexible Forearm," *Proceedings of 1989 American Control Conference*, Pittsburgh, PA, June, pp.1381-1388.

[6] Yang, Y. P. and Huang, K. CM., 1989, "Stochastic Adaptive Control of a Two-Link Manipulator with One Flexible Forearm," *The 13th National Symposium on Automatic Control*, National Taiwan Univ., Taipei, Taiwan, pp.28-36.

[7] Sundararajan, N. and Montgomery, R. C., 1985, "Adaptive Modal Control of Structural Dynamics Systems Using Least-Squares Lattice Filters," *AIAA Journal of Guidance, Control, and Dynamics*, Vol. 8, pp.223-229.

[8] Friedlander, B., 1980, "Recursive Lattice Forms for Adaptive Control," *Proceedings of Joint Automatic Control Conference*, San Francisco, CA, Session WP2-E.

[9] Cetinkunt, S. and Wu, S., 1990, "Tip Position Control of a Flexible One-Arm Robot with Predictive Adaptive Output Feedback Implemented with Lattice Filter Parameter Identifier," *Proceedings IEEE International Conference on Robotics and Automation*, Cincinnati, OH, Vol. 3, pp.1620-1625.

[10] Strobach, P., 1988, "Recursive Covariance Ladder Algorithms for ARMA System Identification," *IEEE Transactions on Acoustics, Speech, and Signal Processing*, Vol. 36, No. 4, April, pp.560-580.

[11] Ling, F. and Proakis, J. G., 1984, "Numerical Accuracy and Stability: Two Problems Caused by Round-Off Error," *Proceedings of International Conference ASSP*, San Diego, CA, pp.30.3.1-30.3.4.

[12] Jabbari, F. and Gibson, J. S., 1988, "Vector-Channel Lattice Filters and Identification of Flexible Structures," *IEEE Transactions on Automatic Control*, Vol. 33, No. 5, May, pp.448-456.

[13] Yang, Y. P., 1988, *Adaptive Control of Robotic Manipulators with Flexible Links*, Ph.D. Dissertation, University of California, Los Angeles.

[14] Ölçer, S., Egardt, B. and Morf, M., 1986, "Convergence Analysis of Ladder Algorithms for AR and ARMA Models," *Automatica*, Vol. 22, No. 3, pp.345-354.

[15] Seraji, H., 1986, "Design of Multivariable Controllers for Robot Manipulators," *Proceedings of 1986 American Control Conference*, Vol. 3, pp.1736-1741.

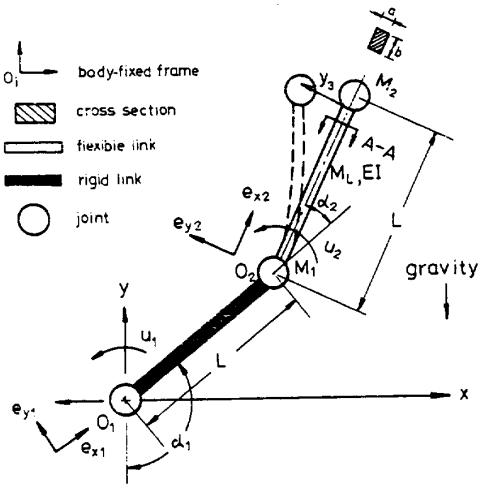

Fig. 1 Two-link robotic manipulator

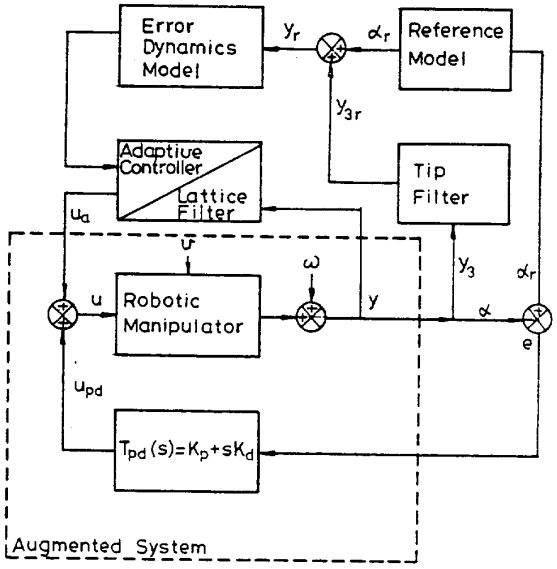

Fig. 2 Closed-loop control system

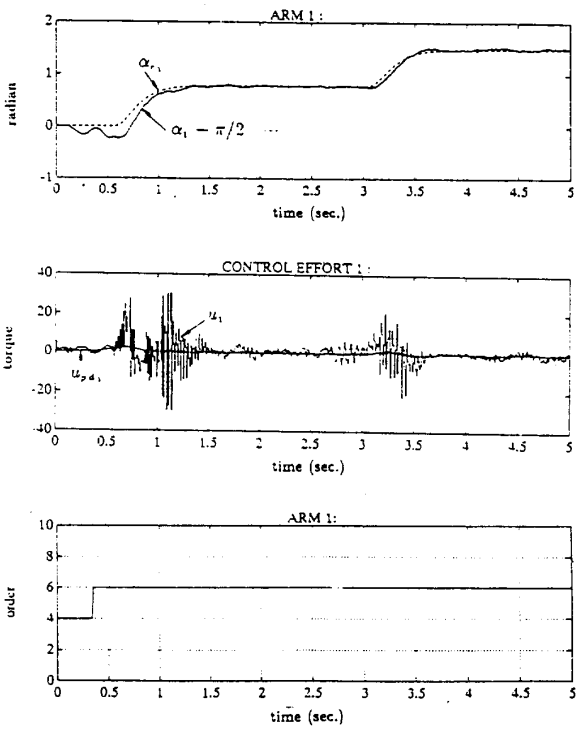

Fig. 3 Control performance of rigid link, M_2=0 before 3 sec., M_2=0.4 m from 3 to 5 sec.

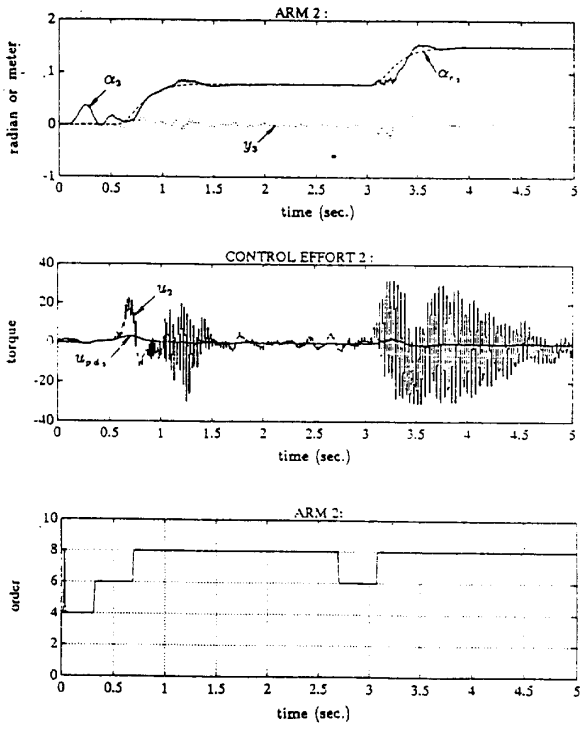

Fig. 4 Control performance of flexible link, M_2=0 before 3 sec., M_2=0.4 m from 3 to 5 sec.